

Biological activity and DNA binding studies of 2-substituted benzimidazo[1,2-*a*]quinolines bearing different amino side chains

Cite this: *Med. Chem. Commun.*, 2013, **4**, 1537

Nataša Perin,^a Irena Martin-Kleiner,^b Raja Nhili,^c William Laine,^c Marie-Hélène David-Cordonnier,^c Oliver Vugrek,^b Grace Karminski-Zamola,^a Marijeta Kralj^{*b} and Marijana Hranjec^{*a}

This manuscript describes the synthesis and biological activity of 2-substituted benzimidazo[1,2-*a*]quinolines substituted with different amino side chains on the quinoline nucleus prepared by microwave assisted amination. The majority of compounds were newly synthesized and active at submicromolar IC₅₀ concentrations, while the alkylamino substituents, either acyclic or cyclic, increased antitumor activities in comparison with previously published nitro and amino substituted benzimidazo[1,2-*a*]quinolines. The compound with the longest tertiary amino side chain (**16**) was the least active. A series of additional experiments, including DNA binding propensities, topoisomerases I and II inhibition, inhibition of recombinant green fluorescent protein in a cell-free translation system, cell cycle perturbances and cellular localization, was performed to shed more light on the mechanisms of action of the most active compounds. The DNA intercalation activity correlates with anti-proliferative effect. Several DNA intercalators (**11**, **20** and **21**) also evidence some sequence selective DNA binding. However, only *N,N*-dimethylaminopropyl analogue **11** was unequivocally demonstrated to be a strong DNA-binder and intercalative agent, which efficiently targets DNA in the cells, while the activity of compound **10**, with a bulky *i*-butylamino side chain, points to its potential antimitotic activity.

Received 10th July 2013
Accepted 18th September 2013

DOI: 10.1039/c3md00193h

www.rsc.org/medchemcomm

Introduction

The permanent and growing interest in the synthesis of benzannulated benzimidazole derivatives, one of the most extensively studied classes of heterocyclic compounds, is a direct consequence of their diverse biological properties.^{1–4} Since benzimidazole exhibits structural similarity with some naturally occurring compounds, their derivatives play a crucial role in the function of some biologically important molecules or can easily interact with biomolecules like DNA, RNA or different proteins of the living systems.^{5,6} DNA still represents one of the principal targets in drug development strategies designed to produce novel therapeutics for diseases such as cancer.⁷ An understanding of the molecular basis of interactions of small heteroaromatic organic molecules with DNA is a promising approach, which is of utmost importance in the rational

development of novel, more selective anticancer agents.⁸ Benzannulated benzimidazoles usually possess a highly conjugated, planar chromophore, which imparts them the ability to intercalate between adjacent DNA base pairs.^{9–11} Due to high fluorescence intensity and excellent spectroscopic characteristics, fused benzimidazoles offer a potential application as fluorescent probes for detection of biologically important molecules such as DNA or proteins in biomedical diagnostics.^{12–14} Recently, as part of our continuous scientific research in the field of potential biologically active benzimidazoles, we have reported on the synthesis and biological activity of several groups of benzimidazo[1,2-*a*]quinolines, including positively charged amidino-substituted benzimidazo[1,2-*a*]quinolines and their heteroaromatic analogues as well as versatile benzimidazo[1,2-*a*]quinolines-6-carbonitriles.^{2,3,15} Biological studies confirmed the anticancer potential of this class of compounds, especially that of positively charged amidino-substituted analogues of benzimidazo[1,2-*a*]quinolines, which intercalate into double-stranded DNA or RNA. The most active one, 2-imidazoliny-substituted benzimidazo[1,2-*a*]quinoline with pronounced selectivity towards colon carcinoma cells, inhibited topoisomerase II and induced strong G2/M cell cycle arrest. On the other hand, uncharged amino- and positively charged diamino-substituted benzimidazo[1,2-*a*]quinolines

^aDepartment of Organic Chemistry, Faculty of Chemical Engineering and Technology, University of Zagreb, Marulićev trg 20, P. O. Box 177, HR-10000 Zagreb, Croatia. E-mail: mhranjec@fkit.hr; Fax: +385 14597250; Tel: +385 14597245

^bDivision of Molecular Medicine, Ruđer Bošković Institute, Bijenička cesta 54, P. O. Box 180, HR-10000 Zagreb, Croatia. E-mail: marijeta.kralj@irb.hr; Fax: +385 1 4561 010; Tel: +385 1 4571 235

^cINSERM U837, Jean-Pierre Aubert Research Centre (JPARC), Team "Molecular and Cellular Targeting for Cancer Treatment", Institut pour la Recherche sur le Cancer de Lille, Université Lille 2, IMPRT-IFR-114, France

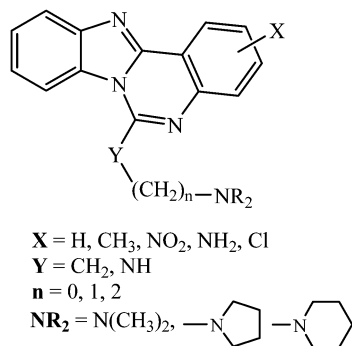


Fig. 1 Amino substituted benzimidazo[1,2-c]quinazolines prepared by Braña *et al.*¹⁷

weakly interact with DNA by partial intercalating or agglomerating along the DNA double helix.^{16b} A fluorescence microscopy study showed cytoplasmic distribution of the compounds, demonstrating that DNA is not their primary target. Benzimidazo[1,2-*a*]quinolines, substituted with piperidine, pyrrolidine and piperazine nuclei were prepared in order to study their spectroscopic properties, especially fluorescence intensity in the presence of CT-DNA. Results revealed significantly enhanced fluorescence emission and thus offer potential applications of those compounds as DNA-specific fluorescent probes.¹³ Another group has published the synthesis of amino-substituted benzimidazo[1,2-*c*]quinazolines with different lengths of amino side chains designed from comparison with other intercalator patterns.¹⁶ All tested compounds showed high cytotoxic activities against several human tumor cell lines.

6-(1-Piperidyl)-ethylamino-substituted derivative with longest side chain showed the highest activity against human osteogenic sarcoma MG-63 in nanomolar concentration, IC_{50} 30 nM (Fig. 1). DNA-binding study reveals intercalation of this near-planar chromophore.

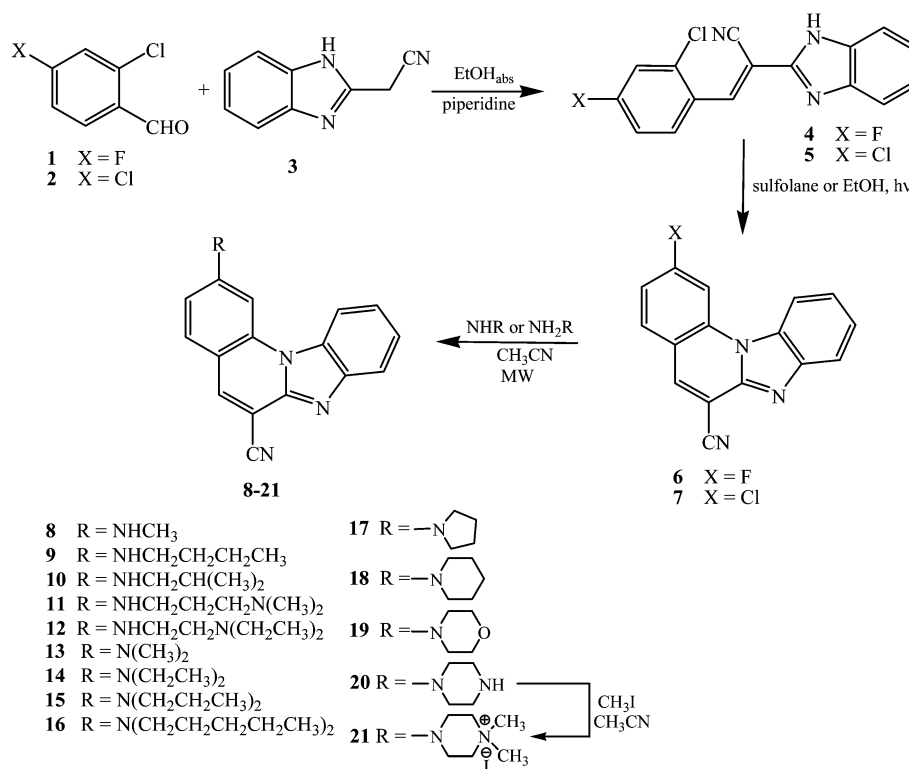
Prompted by the results from those previously reported studies, we set out to explore and synthesize 2-substituted benzimidazole[1,2-*a*]quinolines with different amino substituents on the quinoline nucleus of the condensed tetracyclic ring. All synthesized compounds were tested for their antiproliferative activity *in vitro* against a panel of several human tumor cell lines while compounds **10**, **11**, **20** and **21** were chosen for additional biological studies. A DNA-binding study as well as topoisomerase I and II inhibition was performed for compounds **10**, **11**, **16** and **18–21**.

Results and discussion

Chemistry

All prepared 2-substituted benzimidazo[1,2-*a*]quinolines **8–21** with different amino side chains were synthesized by a microwave assisted amination reaction according to the main synthetic procedure shown in Scheme 1.

Fused starting precursors **6** and **7** were prepared using a previously described method, by a photochemical dehydrohalogenation of non-fused *E*-2-(2-benzimidazolyl)-3-(4-halophenyl)acrylonitriles **4** and **5**, which were prepared by the conventional aldol condensation of 2-cyanomethylbenzimidazole **3** with 4-halobenzaldehydes **1** and **2**.^{3,14} Amino-substituted derivatives **8–20** were prepared in moderate to high yield



Scheme 1 Synthesis of amino substituted benzimidazo[1,2-*a*]quinolines **8–21**.

33–99%. Based on the series of experiments which were undertaken in order to optimize the reaction times and yields, the amination reactions were conducted using 800 W power at 170 °C in acetonitrile with a five to sevenfold excess of the amine.¹⁴ Among all prepared compounds, three compounds were previously prepared in our scientific group,¹⁴ while one compound was previously prepared by another group of authors.¹⁸ The structures of all prepared compounds were determined by NMR analysis based on H–H coupling constants as well as chemical shifts (Table 1) and by mass spectrometry. The ¹H NMR spectra of amino-substituted benzimidazo[1,2-*a*]-quinolines **8–20** showed a downfield shift of the aromatic protons in comparison to 2-fluoro(2-chloro)benzimidazo[1,2-*a*]-quinoline-6-carbonitriles **6** and **7** and the appearance of protons related to amino substituents in the aliphatic region of the NMR spectra between 4.01 and 0.97 ppm. The ¹H NMR spectra of tertiary amino-substituted derivatives **13–16** showed a downfield shift of the H-1, H-3, H-4 and H-5 protons of the quinoline part of the molecule. The same influence on the chemical shifts of H-1, H-3, H-4 and H-5 protons accompanied the introduction of cyclic amino substituents in compounds **18–20**.

N,N-Dimethylated compound **21** as an iodide salt was prepared from piperazinyl substituted benzimidazo[1,2-*a*]-quinoline **20** with an excess of methyl iodide. An attempt to prepare a monomethylated piperazinyl substituted benzimidazo[1,2-*a*]quinoline with an equimolar amount of methyl iodide was not successful. The structure of compound **21** was confirmed by using 2D NMR spectroscopy based on NOE

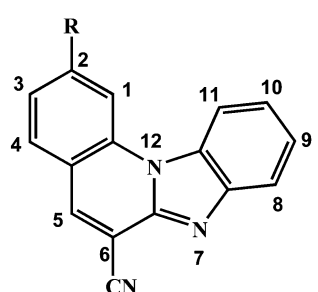
interactions of specific protons of both methyl groups, which showed only mutual NOE interaction as well as interactions with protons of the piperazine nucleus. Introduction of the *N,N*-dimethylated piperazine nucleus as an iodide salt in compound **21** caused a downfield shift of the all aromatic protons in comparison to other amino-substituted derivatives **8–20**.

Biological results and discussion

The tested compounds showed different, but mostly prominent antiproliferative effects on the tested panel cell lines. The length and the type of amino side chains significantly affected antiproliferative activity. Compound **8**, which has the shortest secondary methylamino side chain, showed modest activity, but pronounced selectivity to MCF-7 cells. Although long lipophilic alkyl substituents play an important role on cell penetration and distribution, unexpectedly the compound with the longest tertiary amino side chain (**16**) is the least active compound, which might be due to its lower water solubility caused by its high lipophilicity ($\log P = 8.33$, calculated by ChemDraw 6 software), or steric hindrance. All other compounds have IC₅₀ concentrations in the micromolar (**9**, **14** and **18**), or sub-micromolar range. Still, it should be pointed out that compound **9** formed precipitates, which severely obstructed the MTT assay, therefore, these results should not be correlated with others (Table 2).

Structure–activity relationship (SAR) studies indicated that a secondary amine chain is generally preferred over a tertiary amine chain, although *N,N*-dipropyl-substituted compound **15** showed prominent antiproliferative activity against HCT116 and H460 cells. Compounds substituted with cyclic tertiary amino substituents **19** and **20** also showed prominent antiproliferative activity with the exception of piperidinyl-substituted derivative **18**, which could be explained by the presence of another O or N heteroatom that could contribute

Table 1 ¹H NMR chemical shifts of aromatic protons of compounds **8–21**



Comp.	¹ H NMR (δ /ppm)							
	H-1	H-3	H-4	H-5	H-8	H-9	H-10	H-11
8	7.67	6.90	7.83	8.48	7.94	7.61–7.52	7.61–7.52	8.52
9	7.74	6.91	7.81	8.46	7.94	7.57	7.54	8.52
10	7.80	6.94	7.82	8.47	7.95	7.57	7.53	8.54
11	7.76	6.92	7.80	8.46	7.95	7.58	7.53	8.53
12	7.80	6.95	7.82	8.48	7.95	7.59	7.53	8.60
13	7.51	7.07	7.88	8.53	7.96	7.59	7.52	8.48
14	7.56	7.08	7.88	8.51	7.96	7.57	7.54	8.40
15	7.51	7.06	7.85	8.49	7.96	7.60–7.53	7.60–7.53	8.34
16	7.54	7.06	7.88	8.52	7.97	7.59	7.52	8.37
17	7.44	6.95	7.90	8.54	7.95	7.61–7.52	7.61–7.52	8.51
18	7.79	7.30	7.90	8.56	7.97	7.59	7.54	8.52
19	7.73	7.27	7.89	8.52	7.96	7.59	7.53	8.49
20	7.66	7.24	7.83	8.54	7.94	7.58	7.52	8.43
21	7.92	7.44	8.03	8.66	8.05	7.65	7.59	8.67

Table 2 IC₅₀^a values (in μ M)

Compound	Cell lines		
	HCT116	MCF-7	H460
8 ^{bc}	>10	0.2 ± 0.1	>10
9 ^{cd}	4 ± 0.9	1 ± 0.2	2 ± 0.2
10	0.6 ± 0.01	0.4 ± 0.1	0.3 ± 0.05
11	0.23 ± 0.05	0.4 ± 0.1	0.3 ± 0.1
12	0.2 ± 0.01	0.3 ± 0.02	0.2 ± 0.09
14 ^c	2 ± 0.03	2 ± 1.4	1.6 ± 0.5
15 ^{bc}	0.5 ± 0.02	2.5 ± 1	0.3 ± 0.01
16 ^b	>10	39 ± 13	>10
18 ^c	8 ± 4	2 ± 0.9	5 ± 0.4
19 ^{bc}	0.3 ± 0.09	0.2 ± 0.04	0.3 ± 0.05
20	0.06 ± 0.04	0.2 ± 0.001	0.2 ± 0.03
21 ^b	0.6 ± 0.04	2.4 ± 1.5	2 ± 0.4

^a IC₅₀; the concentration that causes 50% growth inhibition as assessed by MTT assay following 72 hours of incubation. ^b The highest tested concentration was 10 μ M. ^c Compounds were dissolved in DMSO to a stock solutions concentration of 1×10^{-3} to 4×10^{-2} M. However, the precipitation in the cell culture medium at 10^{-4} M after 72 hours was observed. ^d The precipitates interfered with the MTT test.

to interactions with potential biological targets. In compound **21**, one of the piperazine N atoms was quaternized to evaluate the effect of positive permanent charge on the antiproliferative activity and, based on the obtained results, it can be revealed that the antiproliferative activity decreased. The decrease in antiproliferative activity is probably due to the fact that the N heteroatom has lost the ability to interact with potential biological targets because of the steric hindrance of two attached methyl groups. Since there is in general no significant difference in the IC_{50} concentrations between the activity of the most active compounds (e.g. **10** and **11**), while at the same time compound **20** and its iodide salt **21** exert drastically different activities, we attempted flow cytometry analysis of potential cell cycle perturbations in HCT116 cells after the treatment with *i*-butyl substituted derivative **10**, *N,N*-dimethylamino-propyl substituted derivative **11**, piperazinyl-substituted derivative **20** and its *N,N*-dimethyl-substituted iodide salt **21** (Tables 3 and 4).

We tested the effects of various concentrations (0.1, 0.5, 1 and 5 μ M) after 24 and 48 h incubation; however, except for compound **21**, significant effects were seen even at the 0.1 μ M, which are still lower than their IC_{50} concentrations obtained in the MTT test. The results demonstrated that the compounds **10**, **11** and **20** drastically reduced the number of cells in the S phase and induced severe G2/M phase arrest, indicating impairment in progress to mitosis. Also, the concentration-dependant activation of apoptosis can be observed (the SubG1 phase), which goes up to 40% after treatment with 5 μ M concentration of compounds (data not shown). These results suggest that DNA might be the main target of compounds **10**, **11** and **20**. Interestingly, compound **21** did not cause any effect up to the concentration of 5 μ M and 48 h of incubation, when it caused a very slight delay of the cell cycle progression in G1 phase, pointing to a completely different mechanism of action (Table 4).

Table 3 The effects of compounds **10**, **11** and **20** at 0.1 and 1 μ M concentrations on the cell cycle distribution of HCT116 cells after 24 and 48 h treatments. The numbers represent the percentages of cells in the respective cell cycle phase (G1, S and G2/M), along with the percentage of cells in the SubG1 (dead/apoptotic cells) obtained by flow cytometry

Treatment		Percentage of cells (%)			
		SubG1	G1	S	G2/M
24 h	Control	2 ± 0.1	23 ± 2	48 ± 6	29 ± 8
	10 , 0.1 μ M	4 ± 0.2	14 ± 1	44 ± 1	42 ± 2
	10 , 1 μ M	16 ± 5	7 ± 7	8 ± 11	85 ± 4
	11 , 0.1 μ M	6 ± 1	13 ± 1	47 ± 1	40 ± 2
	11 , 1 μ M	5 ± 0.5	22 ± 8	13 ± 18	65 ± 25
	20 , 0.1 μ M	2 ± 0.3	19 ± 1	1 ± 1	80 ± 2
48 h	20 , 1 μ M	12 ± 9	15 ± 3	0 ± 0	85 ± 3
	Control	5 ± 2	60 ± 2	12 ± 5	28 ± 3
	10 , 0.1 μ M	6 ± 3	62 ± 5	21 ± 6	17 ± 1
	10 , 1 μ M	30 ± 2	10 ± 4	0 ± 0	90 ± 4
	11 , 0.1 μ M	4 ± 1	60 ± 0.1	23 ± 0.3	17 ± 0.3
	11 , 1 μ M	8 ± 0.2	41 ± 1	1 ± 0.1	58 ± 1
20 , 0.1 μ M	11 ± 1	59 ± 3	11 ± 4	30 ± 2	
20 , 1 μ M	12 ± 4	30 ± 2	1 ± 0.3	69 ± 2	

Table 4 The effects of compound **21** at 0.5 and 5 μ M concentrations on the cell cycle distribution of HCT116 cells after 24 and 48 h treatments. The numbers represent the percentages of cells in the respective cell cycle phase (G1, S and G2/M), along with the percentage of cells in the subG1 (dead/apoptotic cells) obtained by flow cytometry

Treatment		Percentage of cells (%)			
		SubG0/G1	G0/G1	S	G2/M
24 h	Control	4 ± 1	33 ± 1	39 ± 0.2	28 ± 1
	21 , 0.5 μ M	6 ± 1	32 ± 0.3	36 ± 3	32 ± 3
	21 , 5 μ M	7 ± 0.3	38 ± 2	33 ± 1	29 ± 4
48 h	Control	4 ± 1	37 ± 2	32 ± 1	31 ± 0.1
	21 , 0.5 μ M	6 ± 2	37 ± 0.3	32 ± 1	31 ± 2
	21 , 5 μ M	5 ± 0.1	43 ± 3	29 ± 3	28 ± 0.1

Influence of compounds on protein synthesis

The effect of alkylation of DNA and RNA (coding for a single protein) by nitrogen mustard was previously shown using rabbit reticulocyte lysate as a translation system *in vitro*.¹⁹ The authors showed that when alkylated DNA was used as the template for coupled transcription and translation, a decreased amount of luciferase protein was detected. In addition, it was demonstrated that alkylation of DNA leads to suppression of green fluorescence protein (GFP) plasmid expression in tumor cells.²⁰ In this study, the A549 cells were transfected with a prealkylated GFP plasmid with *N*-methylquinolinium quinone methide and a significant suppression of GFP protein expression was detected.

In present work we used a new approach to evaluate novel compounds in regard to their reactivity and DNA damaging capacity. To do so we used as a reporter, for the first time to our knowledge, Enhanced Green Fluorescent Protein (EGFP) expression in a cell-free environment with a high-capacity T7 promoter driven *in vitro* translation system. Namely, samples of DNA encoding the EGFP gene were treated with compounds **10**, **11**, **20** and **21** and a range of known DNA-damaging agents, and then subjected to coupled transcription and translation to find a correlation between the effect of DNA damage and the amount of transcribed and subsequently translated gene product. Various DNA-damaging compounds were used for comparison; it is evident that the most pronounced inhibitory effect was obtained with the cross-linking agent cisplatin (94% inhibition) and a strong intercalative agent doxorubicin (79% inhibition) (Fig. 2). Also, the alkylating agent chlorambucil inhibits protein expression to 45%; while on the other hand, camptothecin (CPT) or etoposide (data not shown) did not exert any inhibitory effect ($p > 0.05$). Such results were expected because CPT binds reversibly to DNA-topoisomerase I complexes, but not to the enzyme or DNA alone. Therefore, its toxicity is a result of the induction of DNA-strand breaks in intact cells and in the nuclei but not in purified DNA preparations in the absence of topoisomerase I.²¹ Other tested compounds directly damage DNA (cross-linking, alkylation, intercalation) and thus most likely suppress transcription and translation of protein. Similar results, although in different cell-free systems, were obtained by other authors.^{19,22,23}

Inhibition of EGFP translation

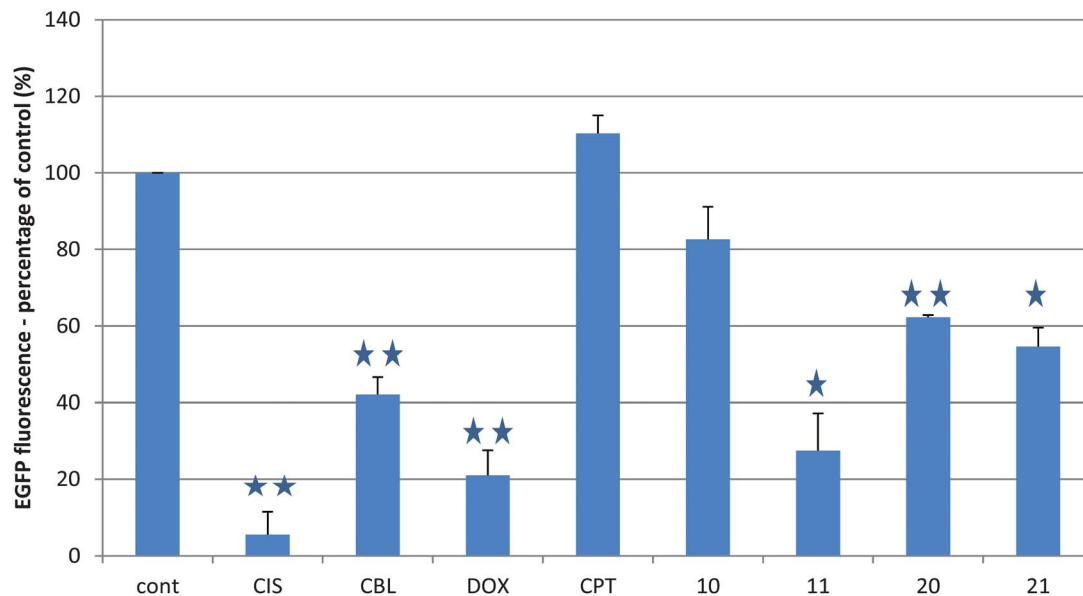


Fig. 2 Inhibition of EGFP protein translation. Plasmid containing EGFP gene under T7 promoter was incubated with compounds **10**, **11**, **20** and **21**, as well as with cisplatin (CIS), chlorambucyl (CBL), doxorubicin (DOX) and camptothecin (CPT) at 50 μM concentrations for 1 h at 24 $^{\circ}\text{C}$. Treated or untreated plasmid was then incubated with the S30 T7 High-Yield Protein Expression System, which enabled the EGFP protein translation/synthesis. The graph represents the percentages of EGFP fluorescence, corresponding to the amount of EGFP protein obtained during the *in vitro* translation procedure. The bars represent average values (\pm sd) of three experiments performed in duplicates. * = $p < 0.05$, ** = $p < 0.005$.

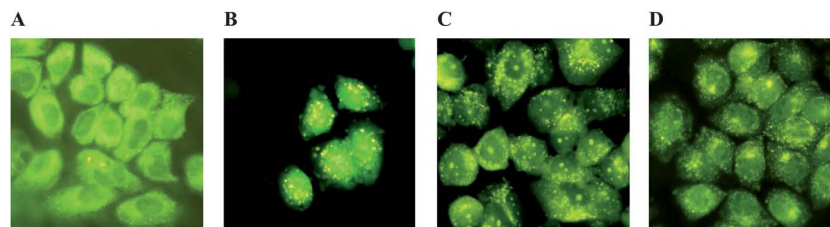


Fig. 3 Fluorescence microscopy images of H460 cells treated with 10 μM concentration of compounds **10** (A), **11** (B), **20** (C) and **21** (D) for 2 h. All compounds, except **11**, show predominantly cytoplasmic distribution (magnification 400 \times).

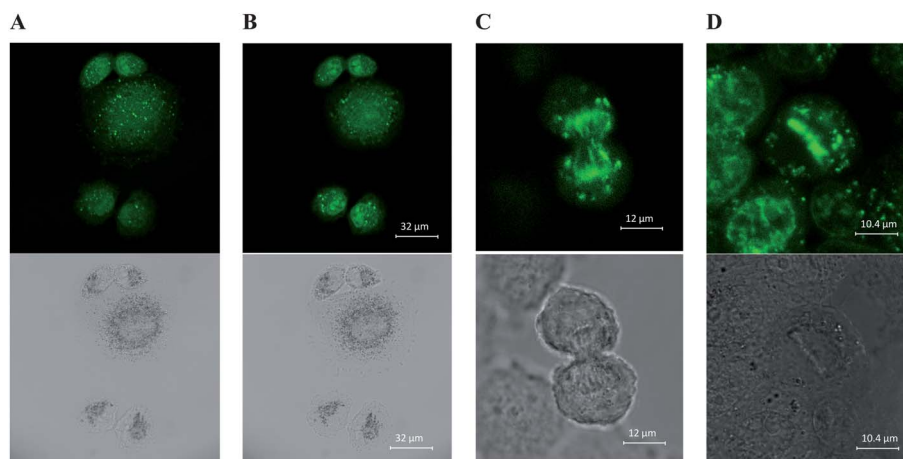


Fig. 4 Confocal laser scanning microscopy of H460 cells treated for 2 h with 10 μM concentration of compound **11**. (A) and (B) represent two optical sections taken at different levels along the z-axis throughout the same cells, (C) and (D) demonstrate intensive staining of mitotic chromosomes. Upper panel – the fluorescence images, excitation at $\lambda_{\text{ex}} = 405$ nm and detection at 424–527 nm; lower panel – the same images in the transmitted light.

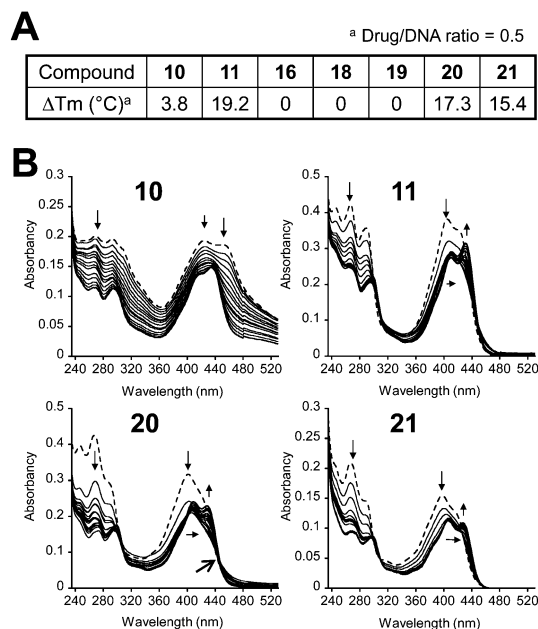


Fig. 5 (A) Variation of DNA melting temperature. (B) UV/visible spectroscopic analyses of the DNA binding of compounds **10**, **11**, **20** and **21**. (B) Spectra of the different compounds (20 μM) alone (dashed lanes) or incubated with graded concentrations of CT-DNA (10, 20, 30, 40, 50, 60, 70, 80, 90, 100, 120, 140, 160, 180, 200 μM ; plain lanes) measured in quartz cuvettes from 230 to 530 nm against a similar cuvette containing the same amount of CT-DNA.

The presented results clearly demonstrate that at DNA level, 50 μM concentrations of all tested compounds inhibit formation of the full-length translated protein. However, the influence of compound **10** is subtle (17% inhibition), but non-significant ($p = 0.1$), pointing to its lower DNA binding/intercalating ability. Compounds **20** and **21** exert intermediate suppression (38% and 45% inhibition, respectively), while compound **11** strongly inhibits EGFP translation (72% inhibition, $p = 0.01$), correlating with its strong DNA-binding and potential intercalative ability.

Subcellular localization of compounds **10**, **11**, **20** and **21**

To check the intracellular distribution of the compounds in the tumor cells, we incubated the H460 cells with the tested compound and performed a fluorescence microscopy study. The H460 cell line was used because the cells are round when attached to the cover slide, have relatively wide cytoplasm and therefore enable better visualization of the intracellular distribution of the compound. Unexpectedly, all compounds show cytoplasmic, mostly punctate staining, pointing to their localization within organelles in the cells and not the nucleus (Fig. 3). Only compound **11** showed both cytoplasmic and nuclear localization (Fig. 3B). Still, there is evidence of differences between the compounds. For example, there is a low general uptake of compound **21** in the cytosol but distinct and somewhat enriched staining in the perinuclear region (Fig. 3D). Similar, but enhanced perinuclear and reticulate fluorescent image of cells treated with compound **20** suggests location at the endoplasmic reticulum (ER), along with a distinctive staining of nucleoli (Fig. 3C). Interestingly, compound **10** showed faint, but very homogenous cytoplasmic staining (Fig. 3A).

Since we noted the remarkable staining pattern of **11**, we also performed laser scanning confocal microscopy to obtain better insight of its localization (Fig. 4).

Interestingly, we observed the accumulation of fluorescence forming cytoplasmic aggregates (Fig. 4A), which could suggest their localization in the lysosomes, or endosomes, along with nuclear staining (Fig. 4B), while in the mitotic cells intensive staining of mitotic chromosomes is evident, confirming its affinity towards DNA (Fig. 4C and D). Further co-localization studies should be performed to confirm the localization in particular organelles.

DNA binding properties

Based on cellular distribution, a selection of compounds from this series was evaluated *in vitro* for DNA binding properties.

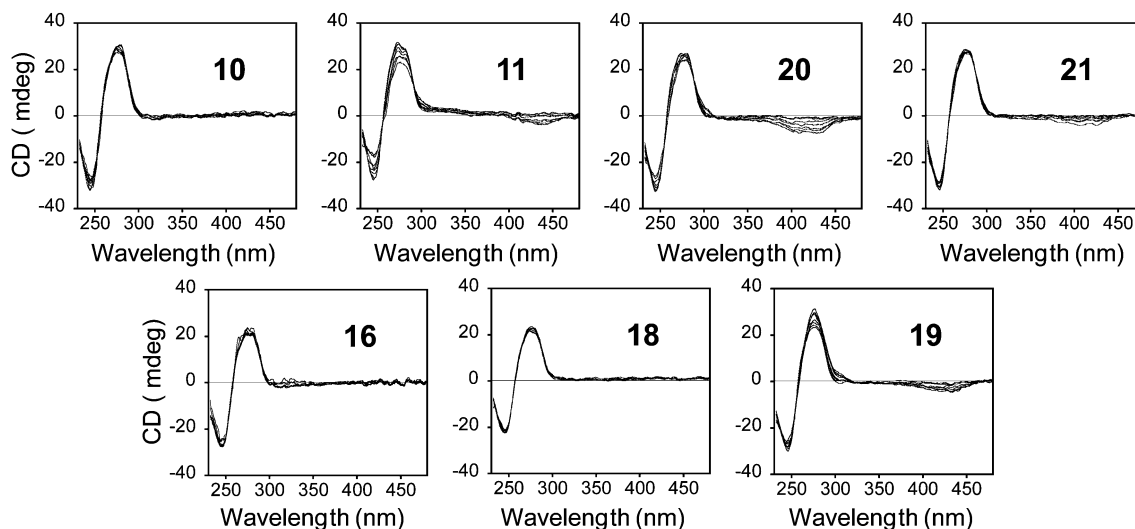


Fig. 6 Circular dichroism spectra of a fixed concentration of CT-DNA (50 μM) incubated with increasing concentrations of compounds **11**, **20** or **21** (1, 5, 10, 20, 30, 40 and 50 μM) are recorded from 230 to 480 nm. Each spectrum is the average of three recordings.

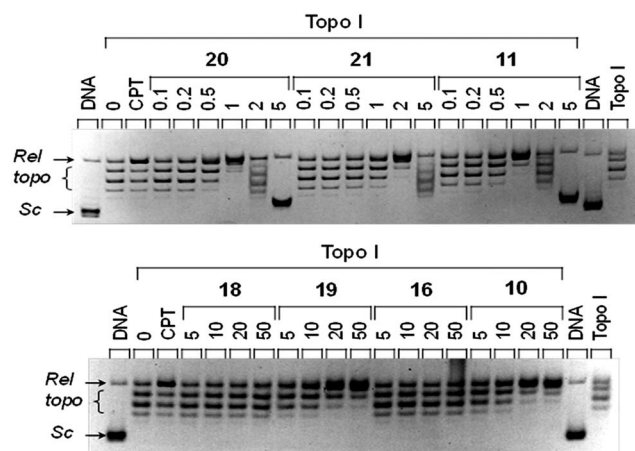


Fig. 7 Topoisomerase I-induced relaxation of the DNA.

The evaluation of the variation of the DNA melting temperature upon the binding of the compounds evidenced compound **10** as a weak DNA binder and compounds **11**, **20** and **21** as strong DNA binders (Fig. 5A).

Compounds **16** and **18**, which were poorly cytotoxic ($>8 \mu\text{M}$), did not stabilize the DNA helix. However, compound **19**, which also failed to stabilize the DNA helix, is cytotoxic in all tested cell lines. UV/visible spectroscopic measurements were performed using a fixed concentration of compounds **10**, **11**, **20** and **21** incubated with increasing concentrations of CT-DNA (Fig. 5B). The results confirm the binding of the four compounds to the DNA with hypochromic (compounds **10**, **11**, **20** and **21**) and bathochromic (compounds **11**, **20** and **21**) effects. The presence of an isosbestic point suggests a single mode of binding.

This mode of binding (intercalation, groove binding) was first investigated using circular dichroism measurements of

CT-DNA upon addition of increasing concentration of the compounds (Fig. 6). The binding of compound **20** to CT-DNA reveals the highest dose-dependent increase of a negative induced-circular dichroism (ICD) within its absorption wavelength (410–440 nm, Fig. 5B). Such negative ICD suggests an intercalation of **20** between adjacent base pairs of the DNA helix. An ICD with much smaller intensity was also observed using compounds **11**, **19** and **21** suggesting less potent intercalative process.

The ICD for compound **11** visualized at 415–440 nm is associated with a decrease of the CD bands associated with the DNA helix (negative peak at 245 nm and positive peak at 280 nm) and is in agreement with an intercalation process that changes the helicity of the DNA. By contrast, compounds **10**, but also **16** and **18** used as control, did not change the CD profile of CT-DNA, suggesting that those compounds do not intercalate into the DNA base pairs.

The intercalation process was confirmed using topoisomerase I-induced relaxation of supercoiled plasmid DNA (Fig. 7).

The typical profile with less and less negatively supercoiled DNA to relaxed DNA and to more and more positively supercoiled plasmid DNA is seen, suggesting the intercalation of the core of the different molecules between adjacent base pairs, resulting in a constrain that favors topoisomerase I-induced relaxation of the supercoiled plasmid to then convert the relaxed form to positively supercoiled circular DNA structures.^{24,25} Only 1 μM (**10**, **20**) or 2 μM (**21**) of compounds is required to fully relax the supercoiled circular plasmid DNA (Rel band). By contrast, compounds **10** and **19** only slightly enhance the topoisomerase I-induced relaxation effect on the global structure of the DNA helix, suggesting that they do not act as intercalating drugs (20–50 μM) and suggesting much weaker intercalative processes as indicated by CD spectra. Compounds

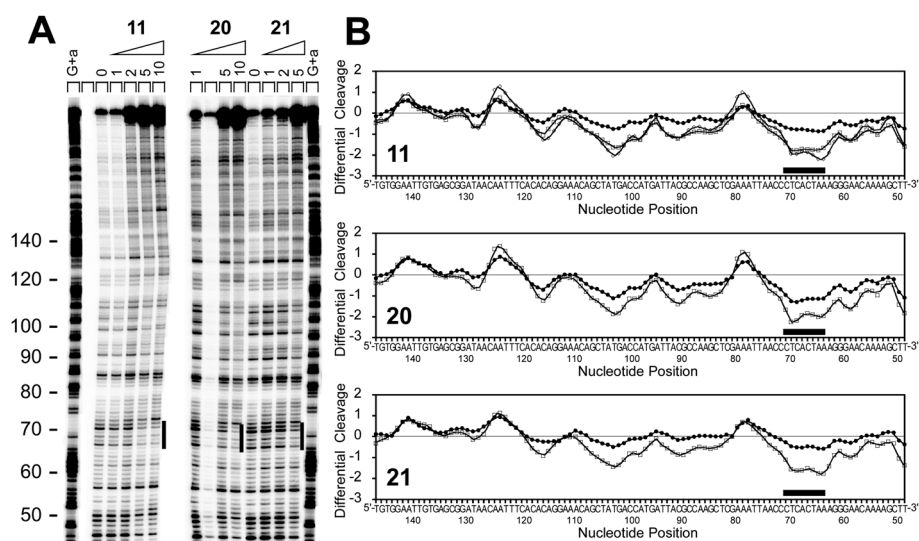


Fig. 8 Sequence-specificity assessed using DNase I footprinting assays. (A) DNase I footprinting gel. The 3'-end radiolabeled 265 bp DNA was incubated with increasing concentrations of compounds **11**, **20** or **21** prior to addition of appropriate concentrations of DNase I enzyme. G+a tracks evidenced guanine and adenine as stronger and weaker bands, respectively, and are obtained from DMS treatment following by hot piperidine cleavage. (B) Densitometric analyses of the gel using compound **11** (2, 5 and 10 μM), **20** (5 and 10 μM) and **21** (2 and 5 μM). Black lanes locate the strongest footprint, both on the gel and on the densitometric spectra.

16 and **18** do not affect the global structure of the DNA helix, suggesting that they do not act as intercalating drugs. Supercoiled pUC19 plasmid DNA (Sc) was incubated with increasing concentrations of the indicated compounds (μM) or CPT as a non-intercalative drug, inducing a nicked DNA that co-migrates with fully relaxed DNA (Rel). Upon treatment with topoisomerase I, a small amount of negatively and then positively supercoiled topoisomers (topo) are evidenced after migration of a 1% agarose gel and post-electrophoresis staining with ethidium bromide. Based on their DNA intercalation ability, the compounds were evaluated for topoisomerases I and II poisoning activities. None of the compounds were able to block cleavable complexes from either topoisomerase I or II (data not shown). We finally looked at potential sequence-selective DNA binding using DNase I footprinting experiments. Only a small selectivity was obtained using the strongest DNA binders **11**, **20** and **21** (Fig. 8).

The covered sections of DNA correspond to the 70-TCCTAA-64 sequence that seems to be covered twice: first at the 70-TCA-68 site and second at the 67-CTAA-64 site. A third and weaker coverage portion is seen at the 110-CTAT-103 site.

Conclusions

This work represents the synthesis of 2-substituted benzimidazo[1,2-*a*]quinolines derivatives **8–21** with different amino side chains placed on the quinoline nucleus with potential chemotherapeutic activities. Amino-substituted compounds were synthesized by uncatalyzed microwave assisted amination from the corresponding chloro(fluoro)-substituted precursor. Benzimidazo[1,2-*a*]quinolines and related benzannulated benzimidazoles, which possess highly conjugated planar chromophores, are well known DNA intercalators while amino chains with different length and flexibility could significantly enhance additional interactions with DNA bases. All compounds showed prominent antiproliferative activity against three tumor cell lines, while the length of the secondary or tertiary amino chains linked to the benzimidazo[1,2-*a*]quinoline nucleus influenced the antiproliferative activity. From this study it has been revealed that the alkylamino substituents, either acyclic or cyclic, increased antitumor activities in comparison with previously published nitro and amino substituted benzimidazo[1,2-*a*]quinolines.¹⁶ Compound **8**, which has the shortest secondary amino side chain, showed modest activity, but pronounced selectivity to MCF-7 cells, while the compound with the longest tertiary amino side chain (**16**) was the least active, probably due to steric hindrance. Although the majority of compounds were active at submicromolar IC_{50} concentrations, we performed a series of additional experiments to shed more light on the mechanisms of action of the most active ones (**10**, **11**, **20** and **21**), including DNA binding propensities, topoisomerases I and II inhibition, cell cycle perturbances and cellular localization. The DNA intercalation activity (as evaluated using topoisomerase I-induced DNA relaxation and circular dichroism) of all tested compounds correlates with the antiproliferative effect since all compounds except **16** and **18** present intercalation profiles with, however, a much lesser

extent obtained by compound **19**. The most efficient DNA intercalators (**10**, **20** and **21**) also evidence some sequence-selective DNA binding. The results were also not completely straightforward, except for *N,N*-dimethylaminopropyl analogue **11**, which was unequivocally demonstrated to be a strong DNA-binder and intercalative agent, which efficiently targets DNA in viable cells. On the other hand, compounds **20** and **21**, despite demonstrating their DNA-binding properties *in vitro* (spectroscopic evaluation, topoisomerase I-mediated DNA relaxation and to some extent the inhibition of protein synthesis *in vitro*), did not confirm the same effects in viable cells. Namely, only **20** demonstrated nuclear staining (more specifically, staining of the nucleoli), while the uptake of quaternary ammonium iodide salt **21** was rather modest and mostly perinuclear staining was observed, accompanied by a poor and completely different influence on the cell cycle. What is more, compound **10** with a bulky *i*-butylamino side chain, although confirmed by all methods not to be a typical intercalator, demonstrated a very pronounced G2/M arrest, along with a drastic S phase reduction, pointing to mitosis inhibition that could be achieved by both DNA intercalation and mitotic spindle-damage. This new series of compounds clearly do not poison topoisomerases I and II (data not shown) even if some compounds strongly bind DNA and intercalate between adjacent base pairs of the DNA helix. However, some sequence-selective DNA binding has been evidenced, corroborating with the EGFP protein translation assays, suggesting some role of DNA targeting in the cellular effect of the compounds. Alternatively, it is possible that it interferes with cellular tubulin polymerization, thus leading to the inhibition of mitotic progression. Finally, we can conclude that *N,N*-dimethylaminopropyl analogue **11** should be further optimized as a lead compound for novel DNA-intercalative compounds, while the *i*-butylamino-substituted benzimidazo[1,2-*a*]quinoline **10** should be tested further to corroborate its antimitotic ability, *i.e.* to test its ability to target microtubules.

Experimental section

General methods

All chemicals and solvents were purchased from commercial suppliers Acros, Aldrich or Fluka. Melting points were recorded on SMP11 Bibby and Büchi 535 apparatus. The ^1H and ^{13}C NMR spectra were recorded on a Varian Gemini 300 or Varian Gemini 600 at 300, 600, 150 and 75 MHz, respectively. All NMR spectra were measured in DMSO-d_6 solutions using TMS as an internal standard. Chemical shifts are reported in ppm (δ) relative to TMS. In preparative photochemical experiments the irradiation was performed at room temperature with a water-cooled immersion well with "Origin Hanau" 400 W high pressure mercury arc lamp using Pyrex glass as a cut-off filter of wavelengths below 280 nm. All compounds were routinely checked by TLC with Merck silica gel 60F-254 glass plates. Mass spectra were recorded on an Agilent 1200 series LC/6410 QQQ instrument. The electronic absorption spectra were recorded on Varian Cary 50 spectrometer using quartz cuvette (1 cm). Elemental analyses for carbon, hydrogen and nitrogen were performed on a Perkin-Elmer 2400 elemental analyzer. Where analyses are

indicated only as symbols of elements, analytical results obtained are within 0.4% of the theoretical value.

Synthesis

2-(2-Benzimidazolyl)-3-(2-chloro-4-fluorophenyl)acrylonitrile

4. Compound **4** was prepared from **3** (1.00 g, 6.37 mmol) and 2-chloro-4-fluorobenzaldehyde **1** (1.00 g, 6.31 mmol) in absolute ethanol (7 ml) after refluxing for 2 h and recrystallization from ethanol to yield 1.41 g (75%) of slightly yellow crystals; mp 234–237 °C; $^1\text{H NMR}$ (300 MHz, DMSO- d_6): δ/ppm = 13.31 (s, 1H, NH_{benzim.}), 8.46 (s, 1H, H_{arom.}), 8.21 (dd, 1H, $J_1 = 6.22$ Hz, $J_2 = 9.07$ Hz, H_{arom.}), 7.74 (dd, 1H, $J_1 = 2.69$ Hz, $J_2 = 8.82$ Hz, H_{arom.}), 7.66 (bs, 2H, H_{benzim.}), 7.51 (dt, 1H, $J_1 = 2.81$ Hz, $J_2 = 8.07$ Hz, H_{benzim.}), 7.30 (bs, 1H, H_{benzim.}); $^{13}\text{C NMR}$ (75 MHz, DMSO- d_6): δ/ppm = 165.28 (s), 161.92 (s), 147.05 (s), 140.69 (d), 135.62 (s), 135.32 (s), 131.93 (d), 128.41 (s), 124.54 (d), 122.97 (d), 119.96 (d), 117.97 (d), 115.80 (s), 115.66 (d), 112.23 (d), 107.16 (s); found: C, 64.81; H, 3.04; N, 6.40. Calc. for C₁₇H₁₂N₄: C, 64.55; H, 3.05; N, 6.38%; MS (ESI): $m/z = 298.1$ ($[\text{M} + 1]^+$).

2-(2-Benzimidazolyl)-3-(2,4-dichlorophenyl)acrylonitrile

5. Compound **5** was prepared from **3** (1.30 g, 8.29 mmol) and 2,4-dichlorobenzaldehyde **1** (1.45 g, 8.29 mmol) in absolute ethanol (10 ml) after refluxing for 2 h and recrystallization from ethanol to yield 1.85 g (71%) of slightly yellow crystals; mp 257–260 °C; $^1\text{H NMR}$ (300 MHz, DMSO- d_6): δ/ppm = 13.32 (s, 1H, NH_{benzim.}), 8.45 (s, 1H, H_{arom.}), 8.15 (d, 1H, $J = 8.46$ Hz, H_{arom.}), 7.89 (d, 1H, $J = 2.10$ Hz, H_{arom.}), 7.69 (dd, 1H, $J_1 = 2.10$ Hz, $J_2 = 8.52$ Hz, H_{arom.}), 7.67 (bs, 1H, H_{benzim.}), 7.27 (bs, 2H, H_{benz.}); $^{13}\text{C NMR}$ (75 MHz, DMSO- d_6): δ/ppm = 146.96 (s), 143.92 (s), 140.62 (d), 140.54 (d), 136.85 (s), 135.31 (s), 131.36 (d), 131.30 (d), 130.71 (s), 130.19 (d), 130.14 (d), 129.78 (d), 128.70 (s), 128.54 (d), 115.68 (s), 107.69 (s); found: C, 61.41; H, 2.88; N, 13.40. Calc. for C₁₇H₁₂N₄: C, 61.17; H, 2.89; N, 13.38%; MS (ESI): $m/z = 314.1$ ($[\text{M} + 1]^+$).

2-Fluorobenzimidazo[1,2-*a*]quinoline-6-carbonitrile

6. Compound **4** (0.50 g, 1.68 mmol) was dissolved in 4 ml of sulfolane and the reaction mixture was heated for 25 minutes at 280 °C. The cooled mixture was poured into water (15 ml), and the resulting product was filtered off and recrystallized from ethanol (450 ml) to obtain a yellow powder (0.32 g, 72%); mp 250–254 °C; $^1\text{H NMR}$ (300 MHz, DMSO- d_6): δ/ppm = 8.77 (s, 1H, H_{arom.}), 8.71 (d, 1H, $J = 8.25$ Hz, H_{arom.}), 8.52 (dd, 1H, $J_1 = 2.10$ Hz, $J_2 = 10.89$ Hz, H_{arom.}), 8.20 (dd, 1H, $J_1 = 6.44$ Hz, $J_2 = 8.42$ Hz, H_{arom.}), 7.99 (d, 1H, $J = 8.21$ Hz, H_{arom.}), 7.61 (t, 1H, $J = 6.82$ Hz, H_{arom.}), 7.58–7.51 (m, 2H, H_{arom.}); $^{13}\text{C NMR}$ (DMSO- d_6) (δ/ppm): 165.48 (s), 163.81 (s), 144.35 (s), 143.63 (s), 140.01 (d), 133.71 (d), 130.22 (s), 125.28 (d), 123.70 (d), 120.13 (d), 118.14 (s), 115.26 (s), 114.83 (d), 113.82 (d), 102.96 (d), 100.33 (s); found: C, 73.27; H, 3.10; N, 16.05. Calc. for C₁₇H₁₂N₄: C, 73.56; H, 3.09; N, 16.00%; MS (ESI): $m/z = 262.1$ ($[\text{M} + 1]^+$).

2-Chlorobenzimidazo[1,2-*a*]quinoline-6-carbonitrile

7. An ethanolic solution (400 ml) of compound **5** (0.90 g, 2.87 mmol) was irradiated at room temperature, with a 400 W high-pressure mercury lamp using a Pyrex filter for 10 h. The obtained product was filtered off to give 0.43 g (54%) of yellow crystals; mp 288–291 °C. $^1\text{H NMR}$ (600 MHz, DMSO- d_6): δ/ppm = 8.80 (s, 1H, H_{arom.}), 8.73 (d, 1H, $J = 7.5$ Hz, H_{arom.}), 8.70 (s, 1H, H_{arom.}), 8.16 (d, 1H, $J =$

8.5 Hz, H_{arom.}), 8.02 (d, 1H, $J = 8.3$ Hz, H_{arom.}), 7.73 (d, 1H, $J = 8.43$ Hz, H_{arom.}), 7.66–7.57 (m, 2H, H_{arom.}); $^{13}\text{C NMR}$ (150 MHz, DMSO- d_6): δ/ppm = 145.04 (s), 142.74 (s), 142.69 (d), 141.02 (s), 139.12 (s), 135.43 (d), 133.05 (s), 128.28 (d), 128.14 (d), 126.74 (d), 122.98 (d), 122.82 (s), 118.06 (d), 117.94 (s), 117.71 (d), 104.19 (s); found: C, 68.99; H, 2.74; N, 15.29. Calc. for C₁₆H₈N₃Cl: C, 69.20; H, 2.90; N, 15.13%; MS (ESI): $m/z = 278.1$ ($[\text{M} + 1]^+$).

General method for preparation of compounds 8–21

Compounds **8–21** were prepared using microwave irradiation, at optimized power and reaction time, from compound **6** or **7** in acetonitrile (10 ml) with an excess of the corresponding amine. After cooling, the reaction mixture was filtered off and resulting product was separated by column chromatography on SiO₂ using dichloromethane–methanol as eluent.

2-*N*-Methylaminobenzimidazo[1,2-*a*]quinoline-6-carbonitrile

8. Compound **8** was prepared using the above described method from **6** (60 mg, 0.23 mmol) and a 33% solution of methylamine in ethanol (0.14 ml, 1.40 mmol) after 4 h of irradiation to yield 61 mg (96%) of yellow crystals; mp > 280 °C. $^1\text{H NMR}$ (300 MHz, DMSO- d_6): δ/ppm = 8.52 (d, 1H, $J = 7.5$ Hz, H-11), 8.48 (s, 1H, H-5), 7.94 (d, 1H, $J = 7.5$ Hz, H-8), 7.83 (d, 1H, $J_1 = 1.7$ Hz, $J_2 = 8.7$ Hz, H-4), 7.67 (s, 1H, H-1), 7.61–7.52 (m, 2H, H-9 and H-10), 7.42 (q, 1H, $J = 4.9$ Hz, NH), 6.90 (dd, 1H, $J_1 = 1.7$ Hz, $J_2 = 8.8$ Hz, H-3), 2.99 (d, 3H, $J = 4.9$ Hz, CH₃); $^{13}\text{C NMR}$ (75 MHz, DMSO- d_6): δ/ppm = 155.06, 146.37, 144.68, 104.55, 138.69, 133.05, 130.87, 125.17 (2C), 122.89 (2C), 119.99, 117.23, 114.94, 111.61, 92.52, 29.78; found: C, 74.90; H, 4.43; N, 20.49. Calc. for C₁₇H₁₂N₄: C, 74.98; H, 4.44; N, 20.58%; MS (ESI): $m/z = 273.1$ ($[\text{M} + 1]^+$).

2-*N*-Butylaminobenzimidazo[1,2-*a*]quinoline-6-carbonitrile

9. Compound **9** was prepared using the above described method from **6** (60 mg, 0.23 mmol) and *n*-butylamine (0.16 ml, 1.60 mmol) after 10 h of irradiation to yield 42 mg (62%) of yellow crystals; mp 234–236 °C. $^1\text{H NMR}$ (300 MHz, DMSO- d_6): δ/ppm = 8.52 (d, 1H, $J = 7.7$ Hz, H-11), 8.46 (s, 1H, H-5), 7.94 (d, 1H, $J = 7.7$ Hz, H-8), 7.81 (d, 1H, $J = 8.8$ Hz, H-4), 7.74 (s, 1H, H-1), 7.57 (dt, 1H, $J_1 = 1.4$ Hz, $J_2 = 8.2$ Hz, H-9), 7.54 (dt, 1H, $J_1 = 1.5$ Hz, $J_2 = 8.2$ Hz, H-10), 7.34 (t, 1H, $J = 5.7$ Hz, NH), 6.91 (d, 1H, $J = 8.7$ Hz, H-3), 1.71–1.61 (m, 2H, CH₂), 1.54–1.42 (m, 4H, CH₂), 0.97 (t, 3H, $J = 7.3$ Hz, CH₃); $^{13}\text{C NMR}$ (150 MHz, DMSO- d_6): δ/ppm = 153.88, 145.91, 144.20, 140.09, 132.78, 130.39, 124.69, 122.36, 119.55 (2C), 116.74, 114.33 (2C), 111.13, 97.54, 91.96, 42.09, 30.49, 19.73, 13.70; found: C, 76.26; H, 5.78; N, 17.77. Calc. for C₂₀H₁₈N₄: C, 76.41; H, 5.77; N, 17.82%; MS (ESI): $m/z = 315.2$ ($[\text{M} + 1]^+$).

2-*N*-*i*-Butylaminobenzimidazo[1,2-*a*]quinoline-6-carbonitrile

10. Compound **10** was prepared using the above described method from **6** (60 mg, 0.23 mmol) and *i*-butylamine (0.11 ml, 1.20 mmol) after 12 h of irradiation to yield 34 mg (47%) of yellow crystals; mp 220–223 °C. $^1\text{H NMR}$ (300 MHz, DMSO- d_6): δ/ppm = 8.54 (dd, 1H, $J_1 = 1.3$ Hz, $J_2 = 7.4$ Hz, H-11), 8.47 (s, 1H, H-5), 7.95 (dd, 1H, $J_2 = 1.3$ Hz, $J_2 = 7.4$ Hz, H-8), 7.82 (d, 1H, $J = 8.8$ Hz, H-4), 7.80 (s, 1H, H-1), 7.57 (dt, 1H, $J_1 = 1.3$ Hz, $J_2 = 7.3$ Hz, H-9), 7.53 (dt, 1H, $J_1 = 1.4$ Hz, $J_2 = 7.3$ Hz, H-10), 7.40 (t, 1H, $J = 5.5$ Hz, NH), 6.94 (dd, 1H, $J_1 = 1.9$ Hz, $J_2 = 8.8$ Hz, H-3), 3.15 (t, 2H, $J = 6.2$ Hz, CH₂), 2.01–1.92 (m, 1H, CH), 1.03 (d, 6H, $J = 6.7$ Hz, CH₃); $^{13}\text{C NMR}$ (75 MHz, DMSO- d_6): δ/ppm = 154.55,

146.40, 144.69, 138.52, 133.30, 130.88, 125.17, 122.84, 114.80 (2C), 111.61, 92.43, 50.58, 28.11, 20.80 (2C); found: C, 76.48; H, 5.75; N, 17.83. Calc. for $C_{20}H_{18}N_4$: C, 76.41; H, 5.77; N, 17.82%; MS (ESI): $m/z = 315.2$ ($[M + 1]^+$).

2-[*N,N*-Dimethylaminopropyl-1-amino]benzimidazo[1,2-*a*]quinoline-6-carbonitrile 11. Compound 11 was prepared using the above described method from **6** (120 mg, 0.46 mmol) and *N,N*-dimethylaminopropyl-1-amine (0.33 ml, 2.30 mmol) after 6 h of irradiation to yield 120 mg (76%) of yellow crystals; mp 185–187 °C. 1H NMR (600 MHz, DMSO- d_6): $\delta/ppm = 8.53$ (d, 1H, $J = 8.3$ Hz, H-11), 8.46 (s, 1H, H-5), 7.95 (d, 1H, $J = 8.2$ Hz, H-8), 7.80 (d, 1H, $J = 8.8$ Hz, H-4), 7.76 (s, 1H, H-1), 7.58 (dt, 1H, $J_1 = 1.1$ Hz, $J_2 = 7.5$ Hz, H-9), 7.53 (dt, 1H, $J_1 = 1.3$ Hz, $J_2 = 7.4$ Hz, H-10), 7.38 (t, 1H, $J = 5.4$ Hz, NH), 6.92 (dd, 1H, $J_1 = 1.9$ Hz, $J_2 = 8.8$ Hz, H-3), 3.37 (q, 2H, $J = 6.6$ Hz, CH_2), 2.37 (t, 2H, $J = 6.7$ Hz, CH_2), 2.18 (s, 6H, CH_3), 1.82–1.78 (m, 2H, CH_2); ^{13}C NMR (75 MHz, DMSO- d_6): $\delta/ppm = 164.06$, 154.41, 146.41, 144.70, 140.56, 133.21, 130.88, 125.20 (2C), 122.83 (2C), 120.03, 117.24, 114.86, 111.63, 92.46, 56.94 (2C), 45.74 (2C), 27.15; found: C, 73.66; H, 6.14; N, 20.36. Calc. for $C_{21}H_{21}N_5$: C, 73.44; H, 6.16; N, 20.39%; MS (ESI): $m/z = 344.2$ ($[M + 1]^+$).

2-[*N,N*-Diethylethylenediamino]benzimidazo[1,2-*a*]quinoline-6-carbonitrile 12. Compound 12 was prepared using the above described method from **6** (60 mg, 0.23 mmol) and *N,N*-diethylethylenediamine (0.20 ml, 1.40 mmol) after 2 h of irradiation to yield 40 mg (44%) of yellow crystals; mp 183–186 °C. 1H NMR (600 MHz, DMSO- d_6): $\delta/ppm = 8.60$ (d, 1H, $J = 8.3$ Hz, H-11), 8.48 (s, 1H, H-5), 7.95 (d, 1H, $J = 8.2$ Hz, H-8), 7.82 (d, 2H, $J = 8.7$ Hz, H-4), 7.80 (s, 1H, H-1), 7.59 (dt, 1H, $J_1 = 1.2$ Hz, $J_2 = 7.3$ Hz, H-9), 7.53 (dt, 1H, $J_1 = 1.2$ Hz, $J_2 = 7.3$ Hz, H-10), 7.27 (t, 1H, $J = 5.0$ Hz, NH), 6.95 (dd, 1H, $J_1 = 1.9$ Hz, $J_2 = 8.8$ Hz, H-3), 3.42 (q, 2H, $J = 6.5$ Hz, CH_2), 2.70 (t, 2H, $J = 6.6$ Hz, CH_2), 2.6 (q, 4H, $J = 7.1$ Hz, CH_2), 1.01 (t, 6H, $J = 7.1$ Hz, CH_3); ^{13}C NMR (150 MHz, DMSO- d_6): $\delta/ppm = 153.80$, 145.91, 144.22, 140.01, 138.13, 132.68, 130.40, 124.68, 122.28, 119.52, 116.69, 114.46, 111.24, 92.15, 51.39, 46.58 (2C), 41.15 (2C), 11.61 (2C); found: C, 74.07; H, 6.47; N, 19.66. Calc. for $C_{22}H_{23}N_5$: C, 73.92; H, 6.49; N, 19.59%; MS (ESI): $m/z = 358.2$ ($[M + 1]^+$).

2-*N,N*-Dimethylaminobenzimidazo[1,2-*a*]quinoline-6-carbonitrile 13. Compound 13 was prepared using the above described method from **7** (50 mg, 0.18 mmol) and 33% solution of dimethylamine in ethanol (0.18 ml, 0.90 mmol) after 16 h of irradiation to yield 30 mg (61%) of yellow crystals; mp > 280 °C. 1H NMR (300 MHz, DMSO- d_6): $\delta/ppm = 8.53$ (s, 1H, H-5), 8.48 (d, 1H, $J = 7.8$ Hz, H-11), 7.96 (d, 1H, $J = 7.8$ Hz, H-8), 7.88 (d, 1H, $J = 9.1$ Hz, H-4), 7.59 (dt, 1H, $J_1 = 1.9$ Hz, $J_2 = 7.3$ Hz, H-9), 7.52 (dt, 1H, $J_1 = 1.9$ Hz, $J_2 = 7.3$ Hz, H-10), 7.51 (s, 1H, H-1), 7.07 (dd, 1H, $J_1 = 2.1$ Hz, $J_2 = 9.1$ Hz, H-3), 3.26 (s, 6H, CH_3); ^{13}C NMR (150 MHz, DMSO- d_6): $\delta/ppm = 153.41$, 145.83, 144.16, 139.89, 138.02, 132.22, 130.28, 124.74, 119.54, 116.61, 114.59, 110.90, 110.64, 95.25, 92.76, 40.05 (2C); found: C, 75.73; H, 4.92; N, 19.51. Calc. for $C_{18}H_{14}N_4$: C, 75.50; H, 4.93; N, 19.57%; MS (ESI): $m/z = 287.1$ ($[M + 1]^+$).

2-*N,N*-Diethylaminobenzimidazo[1,2-*a*]quinoline-6-carbonitrile 14. Compound 14 was prepared using the above described method from **6** (60 mg, 0.23 mmol) and a 70% solution of diethylamine in ethanol (0.17 ml, 1.60 mmol) after 19 h of

irradiation to yield 60 mg (80%) of yellow crystals; mp 197–199 °C. 1H NMR (300 MHz, DMSO- d_6): $\delta/ppm = 8.51$ (s, 1H, H-5), 8.40 (dd, 1H, $J_1 = 1.8$ Hz, $J_2 = 7.2$ Hz, H-11), 7.96 (dd, 1H, $J_1 = 1.8$ Hz, $J_2 = 7.2$ Hz, H-8), 7.88 (d, 1H, $J = 9.2$ Hz, H-4), 7.57 (dt, 1H, $J_1 = 2.2$ Hz, $J_2 = 7.3$ Hz, H-9), 7.56 (s, 1H, H-1), 7.54 (dt, 1H, $J_1 = 2.1$ Hz, $J_2 = 7.2$ Hz, H-10), 7.08 (dd, 1H, $J_1 = 2.3$ Hz, $J_2 = 9.1$ Hz, H-3), 3.67 (q, 4H, $J = 7.1$ Hz, CH_2), 1.28 (t, 6H, $J = 7.1$ Hz, CH_3); ^{13}C NMR (150 MHz, DMSO- d_6): $\delta/ppm = 151.24$, 145.91, 144.21, 139.74, 138.40, 132.57, 130.29, 124.71, 122.70, 119.63, 116.69, 114.05, 110.67, 110.47, 94.78, 92.36, 44.57 (2C), 12.11 (2C); found: C, 76.26; H, 5.78; N, 17.75. Calc. for $C_{20}H_{18}N_4$: C, 76.41; H, 5.77; N, 17.82%; MS (ESI): $m/z = 315.2$ ($[M + 1]^+$).

2-*N,N*-Dipropylaminobenzimidazo[1,2-*a*]quinoline-6-carbonitrile 15. Compound 15 was prepared using the above described method from **6** (90 mg, 0.34 mmol) and dipropylamine (0.24 ml, 1.70 mmol) after 9 h of irradiation to yield 70 mg (60%) of yellow crystals; mp 208–211 °C. 1H NMR (300 MHz, DMSO- d_6): $\delta/ppm = 8.49$ (s, 1H, H-5), 8.34 (d, 1H, $J = 7.8$ Hz, H-11), 7.96 (d, 1H, $J = 7.8$ Hz, H-8), 7.85 (d, 1H, $J = 9.1$ Hz, H-4), 7.60–7.53 (m, 2H, H-9 and H-10), 7.51 (s, 1H, H-1), 7.06 (dd, 1H, $J_1 = 1.9$ Hz, $J_2 = 9.1$ Hz, H-11), 3.57 (t, 4H, $J = 7.6$ Hz, CH_2), 1.77–1.65 (m, 4H, CH_2), 1.00 (t, 6H, $J = 7.3$ Hz, CH_3); ^{13}C NMR (75 MHz, DMSO- d_6): $\delta/ppm = 152.23$, 150.06, 146.44, 144.75, 140.28, 138.82, 132.99, 130.78, 125.24, 123.07, 120.24, 117.18, 114.39, 111.17, 95.56, 92.89, 52.80 (2C), 20.30 (2C), 11.58 (2C); found: C, 77.47; H, 6.46; N, 16.33. Calc. for $C_{22}H_{22}N_4$: C, 77.16; H, 6.48; N, 16.36%; MS (ESI): $m/z = 343.3$ ($[M + 1]^+$).

2-*N,N*-Dipentylaminobenzimidazo[1,2-*a*]quinoline-6-carbonitrile 16. Compound 16 was prepared using the above described method from **6** (60 mg, 0.23 mmol) and dipentylamine (0.24 ml, 1.20 mmol) after 12 h of irradiation to yield 30 mg (33%) of yellow crystals; mp 131–134 °C. 1H NMR (300 MHz, DMSO- d_6): $\delta/ppm = 8.52$ (s, 1H, H-5), 8.37 (d, 1H, $J = 8.1$ Hz, H-11), 7.97 (d, 1H, $J = 7.9$ Hz, H-8), 7.88 (d, 1H, $J = 9.1$ Hz, H-4), 7.59 (t, 1H, $J = 7.6$ Hz, H-9), 7.54 (s, 1H, H-1), 7.52 (t, 1H, $J = 7.6$ Hz, H-10), 7.06 (dd, 1H, $J_1 = 1.9$ Hz, $J_2 = 9.1$ Hz, H-3), 3.60 (t, 4H, $J = 7.7$ Hz, CH_2), 1.74–1.66 (m, 4H, CH_2), 1.44–1.37 (m, 8H, CH_2), 0.92 (t, 6H, $J = 6.9$ Hz, CH_3); ^{13}C NMR (75 MHz, DMSO- d_6): $\delta/ppm = 152.04$, 146.43, 144.75, 140.22, 138.75, 132.95, 130.71, 125.24, 122.79, 120.23, 117.16, 114.33, 111.14, 111.07, 95.44, 92.86, 51.20 (2C), 29.11 (2C), 26.62 (2C), 22.49 (2C), 14.52 (2C); found: C, 78.59; H, 7.57; N, 14.03. Calc. for $C_{26}H_{30}N_4$: C, 78.35; H, 7.59; N, 14.06%; MS (ESI): $m/z = 399.4$ ($[M + 1]^+$).

2-*N*-Pyrrolydinybenzimidazo[1,2-*a*]quinoline-6-carbonitrile 17. Compound 17 was prepared using the above described method from **7** (50 mg, 0.18 mmol) and pyrrolidine (0.07 ml, 0.90 mmol) after 6 h of irradiation to yield 51 mg (90%) of yellow crystals; mp > 295 °C. 1H NMR (600 MHz, DMSO- d_6): $\delta/ppm = 8.54$ (s, 1H, H-1), 8.51 (d, 1H, $J = 7.9$ Hz, H-11), 7.95 (d, 1H, $J = 7.9$ Hz, H-8), 7.90 (d, 1H, $J = 9.0$ Hz, H-4), 7.61–7.52 (m, 2H, H-9 and H-10), 7.44 (s, 1H, H-1), 6.95 (dd, 1H, $J_1 = 1.9$ Hz, $J_2 = 9.0$ Hz, H-3), 3.67 (t, 4H, $J = 6.7$ Hz, CH_2), 2.55 (t, 4H, $J = 6.7$ Hz, CH_2); ^{13}C NMR (150 MHz, DMSO- d_6): $\delta/ppm = 164.63$, 153.15, 147.73, 143.82, 142.99, 138.50, 133.60, 130.78, 127.76, 125.27, 124.20, 122.07, 115.15, 113.08, 112.88, 111.76, 48.37 (2C), 25.45 (2C); found: C, 77.11; H, 5.33; N, 17.82. Calc. for $C_{20}H_{16}N_4$: C, 76.90; H, 5.16; N, 17.94%; MS (ESI): $m/z = 313.4$ ($[M + 1]^+$).

2-N-Piperidinylbenzimidazo[1,2-*a*]quinoline-6-carbonitrile 18.

Compound **18** was prepared using the above described method from **7** (50 mg, 0.18 mmol) and piperidine (0.09 ml, 0.90 mmol) after 6 h of irradiation to yield 45 mg (85%) of yellow crystals; mp 254–256 °C. ¹H NMR (600 MHz, DMSO-*d*₆): δ/ppm = 8.56 (s, 1H, H-5), 8.52 (d, 1H, *J* = 8.2 Hz, H-11), 7.97 (d, 1H, *J* = 8.2 Hz, H-8), 7.90 (d, 1H, *J* = 9.1 Hz, H-4), 7.79 (bs, 1H, H-1), 7.59 (dt, 1H, *J*₁ = 1.4 Hz, *J*₂ = 7.3 Hz, H-9), 7.54 (dt, 1H, *J*₁ = 1.5 Hz, *J*₂ = 7.3 Hz, H-10), 7.30 (dd, 1H, *J*₁ = 1.9 Hz, *J*₂ = 9.2 Hz, H-3), 3.69–3.62 (m, 6H, CH₂), 1.67 (t, 4H, *J* = 6.3 Hz, CH₂), 1.23 (s, 2H); ¹³C NMR (150 MHz, DMSO-*d*₆): δ/ppm = 154.54, 146.27, 144.70, 140.15, 138.82, 132.86, 130.83, 125.27, 123.34, 120.16, 116.90, 115.05, 112.99, 112.31, 97.83, 94.34, 48.57 (2C), 25.46 (2C), 24.23; found: C, 77.55; H, 5.78; N, 17.09. Calc. for C₂₁H₁₈N₄: C, 77.28; H, 5.56; N, 17.17%; MS (ESI): *m/z* = 327.2 ([M + 1]⁺).

2-N-Morpholinylbenzimidazo[1,2-*a*]quinoline-6-carbonitrile 19.

Compound **19** was prepared using the above described method from **6** (60 mg, 0.23 mmol) and morpholine (0.12 ml, 1.40 mmol) after 4 h of irradiation to yield 42 mg (56%) of yellow crystals; mp > 280 °C. ¹H NMR (300 MHz, DMSO-*d*₆): δ/ppm = 8.52 (s, 1H, H-5), 8.49 (d, 1H, *J* = 8.1 Hz, H-11), 7.96 (d, 1H, *J* = 8.1 Hz, H-8), 7.89 (d, 1H, *J* = 9.1 Hz, H-4), 7.73 (s, 1H, H-1), 7.59 (t, 1H, *J* = 7.4 Hz, H-9), 7.53 (t, 1H, *J* = 7.2 Hz, H-10), 7.27 (dd, 1H, *J*₁ = 1.9 Hz, *J*₂ = 9.0 Hz, H-11), 3.85 (t, 4H, *J* = 4.6 Hz, CH₂), 3.56 (t, 4H, *J* = 4.6 Hz, CH₂); ¹³C NMR (75 MHz, DMSO-*d*₆): δ/ppm = 163.16, 154.73, 144.54, 140.32, 138.43, 132.75, 130.74, 125.38, 123.43, 120.19, 116.81, 115.31, 113.20, 112.69, 98.03, 95.21, 66.34 (2C), 42.24 (2C); found: C, 73.44; H, 4.89; N, 17.04. Calc. for C₂₀H₁₆N₄O (326.3): C, 73.15; H, 4.91; N, 17.06%; MS (ESI): *m/z* = 329.2 ([M + 1]⁺).

2-N-Piperazinylbenzimidazo[1,2-*a*]quinoline-6-carbonitrile 20.

Compound **20** was prepared using the above method from **7** (50 mg, 0.18 mmol) and piperazine (780 mg, 0.90 mmol) after 10 h of irradiation to yield 33 mg (56%) of yellow crystals; mp 192–196 °C. ¹H NMR (600 MHz, DMSO-*d*₆): δ/ppm = 8.87 (s, 1H, NH), 8.54 (s, 1H, H-5), 8.43 (d, 1H, *J* = 8.0 Hz, H-11), 7.94 (d, 1H, *J* = 8.0 Hz, H-8), 7.83 (dd, 1H, *J*₁ = 1.2 Hz, *J*₂ = 9.2 Hz, H-4), 7.66 (s, 1H, H-1), 7.58 (t, 1H, *J* = 8.2 Hz, H-9), 7.52 (t, 1H, *J* = 8.2 Hz, H-10), 7.24 (dd, 1H, *J*₁ = 1.3 Hz, *J*₂ = 9.2 Hz, H-3), 3.49 (t, 4H, *J* = 4.5 Hz, CH₂), 2.93 (t, 4H, *J* = 4.5 Hz, CH₂); ¹³C NMR (150 MHz, DMSO-*d*₆): δ/ppm = 154.12, 145.55, 144.03, 139.66, 137.94, 132.17, 130.18, 124.79, 122.85, 119.61, 116.37, 114.67, 112.22, 112.20, 97.33, 94.24, 47.16 (2C), 44.89 (2C); found: C, 73.18; H, 5.15; N, 21.55. Calc. for C₂₀H₁₉N₅: C, 73.37; H, 5.23; N, 21.34%; MS (ESI): *m/z* = 328.3 ([M + 1]⁺).

2-N-(4-N,N-Dimethylpiperazin-1-yl)benzimidazo[1,2-*a*]quinoline-6-carbonitrile iodide 21. A mixture of compound **20** (50 mg, 0.15 mmol) and anhydrous potassium carbonate (21 mg, 0.15 mmol) was refluxed in acetonitrile (20 ml) with methyl iodide (0.03 ml, 0.46 mmol) for 2 h. The reaction mixture was concentrated under reduced pressure to a volume of 5 ml and filtered off to yield pure compound **21** as yellow powder (50 mg, 67%); mp 270–273 °C. ¹H NMR (600 MHz, DMSO-*d*₆): δ/ppm = 8.67 (d, 1H, *J* = 8.4 Hz, H-11), 8.66 (s, 1H, H-5), 8.05 (d, 1H, *J* = 8.4 Hz, H-8), 8.03 (d, 1H, *J* = 8.9 Hz, H-4), 7.92 (s, 1H, H-1), 7.65 (t, 1H, *J* = 7.6 Hz, H-9), 7.59 (t, 1H, *J* = 7.6 Hz, H-10), 7.44 (dd, 1H, *J*₁ = 1.9 Hz, *J*₂ = 8.8 Hz, H-3), 4.01 (t, 4H, *J* =

5.4 Hz, CH₂), 3.70 (t, 4H, *J* = 5.5 Hz, CH₂), 3.30 (s, 6H, CH₃); ¹³C NMR (75 MHz, DMSO-*d*₆): δ/ppm = 153.55, 145.95, 144.57, 140.36, 138.32, 132.92, 130.77, 125.54, 123.56, 120.45, 116.57, 115.44, 113.43, 112.87, 99.26, 96.37, 60.49 (2C), 51.01 (2C), 41.59 (2C); found: C, 54.83; H, 4.58; N, 14.46. Calc. for C₂₂H₂₂IN₅: C, 54.67; H, 4.59; N, 14.49%; MS (ESI): *m/z* = 356.4 ([M – I]⁺).

Antiproliferative evaluation assay

The experiments were carried out on three human cell lines, which are derived from three cancer types. The following cell lines were used: HCT116 (colon carcinoma), H460 (lung carcinoma) and MCF-7 (breast carcinoma). The cells were cultured as monolayers and maintained in Dulbecco's modified Eagle's medium (DMEM) supplemented with 10% fetal bovine serum (FBS), 2 mM l-glutamine, 100 U per ml penicillin and 100 μg per ml streptomycin in a humidified atmosphere with 5% CO₂ at 37 °C.

The growth inhibition activity was assessed as described previously.²¹ The cell lines were inoculated onto a series of standard 96-well microtiter plates on day 0, at 3 × 10⁴ cells per ml (HCT116, H460) to 5 × 10⁴ cells per ml (MCF-7), depending on the doubling times of a specific cell line. Test agents were then added in ten-fold dilutions (10⁻⁸ to 10⁻⁴ M) and incubated for further 72 h. Working dilutions were freshly prepared on the day of testing. After 72 h of incubation the cell growth rate was evaluated by performing the MTT assay, which detects dehydrogenase activity in viable cells. The absorbance (*A*) was measured using a microplate reader at 570 nm. The absorbance is directly proportional to the number of living, metabolically active cells. The percentage of growth (PG) of the cell lines was calculated according to one or the other of the following two expressions:

$$\text{If } (\text{mean } A_{\text{test}} - \text{mean } A_{\text{tzero}}) \geq 0, \text{ then PG} = 100 \times (\text{mean } A_{\text{test}} - \text{mean } A_{\text{tzero}}) / (\text{mean } A_{\text{ctrl}} - \text{mean } A_{\text{tzero}}).$$

If (mean *A*_{test} – mean *A*_{tzero}) < 0, then: PG = 100 × (mean *A*_{test} – mean *A*_{tzero})/*A*_{tzero}, where the mean *A*_{tzero} is the average of optical density measurements before exposure of cells to the test compound, the mean *A*_{test} is the average of optical density measurements after the desired period of time and the mean *A*_{ctrl} is the average of optical density measurements after the desired period of time with no exposure of cells to the test compound. The results are expressed as IC₅₀, which is the concentration necessary for 50% of inhibition. The IC₅₀ values for each compound are calculated from concentration–response curves using linear regression analysis by fitting the test concentrations that give PG values above and below the reference value (*i.e.* 50%). If, however, all of the tested concentrations produce PGs exceeding the respective reference level of effect (*e.g.* PG value of 50), then the highest tested concentration is assigned as the default value, which is preceded by a “>” sign. Each test was performed in quadruplicate in at least two individual experiments.

Cell cycle analysis

Tumor cells were seeded per well into a 6-well plate (2×10^5 per well). After 24 hours the tested compounds were added at various concentrations (as shown in the Results section). After the desired length of time the attached cells were trypsinized, combined with floating cells, washed with phosphate buffer saline (PBS), fixed with 70% ethanol and stored at -20°C . Immediately before the analysis, the cells were washed with PBS and stained with $50 \mu\text{g ml}^{-1}$ of propidium iodide (PI) with the addition of $0.2 \mu\text{g ml}^{-1}$ of RNase A. The stained cells were then analyzed with a FACScalibur (Becton Dickinson) flow cytometer (20 000 counts were measured). The percentage of the cells in each cell cycle phase was determined using the ModFit LT™ software (Verity Software House) based on the DNA histograms. The tests were performed in duplicates and repeated at least twice.

Intracellular distribution of compounds

H460 cells were seeded on round microscopic cover slips placed in 24-well-plates (10 000 cells per well) and grown at 37°C for 24 h in DMEM, as described above. Cells were then incubated with compounds **10**, **11**, **20** and **21** at $10 \mu\text{M}$ final concentrations for 2 h. Cover slips were rinsed twice with PBS, placed on the microscopic slides and immediately analyzed. The uptake and intracellular distribution of tested chemicals were analyzed under a fluorescence microscope (Olympus BX51) and recorded with an Olympus DP70 Digital Camera. Also, confocal laser scanning microscopy was performed using a Leica TCS SP2 AOBs confocal microscope equipped with an HCX PL APO λ -Blue 63 \times /1.4 objective (Leica Microsystems). Fluorescence and transmission images were acquired simultaneously. For illumination, the 405 nm line from an argon-ion gas laser was used and fluorescence was collected in the 424–527 nm range. Confocal fluorescence images were taken using the pinhole size of $114 \mu\text{m}$ (1 Airy unit).

Inhibition of *in vitro* translation

The compounds **10**, **11**, **20** and **21** were tested for inhibitory effect on translation of Enhanced Green Fluorescence Protein (EGFP) using an *E. coli* derived cell-free protein synthesis system (S30 T7 High-Yield Protein Expression System, Promega, USA). It can produce high levels of recombinant proteins if supplemented with an appropriate expression plasmid, T7 RNA polymerase for transcription, and other necessary components for translation such as amino acids. Briefly, 500 ng of pEGFP-C1 plasmid (Clontech, USA) was incubated with the tested compounds (at $50 \mu\text{M}$ concentration) for 1 h at 24°C . Positive controls contained the plasmid in sterile water and negative controls did not contain the DNA template (plasmid), respectively. Along with the tested compounds, commercial DNA-damage-inducing anticancer drugs doxorubicine, camptothecin, cisplatin and chlorambucyl ($50 \mu\text{M}$ concentration, Sigma) were also used for comparison. After that, the protein expression system was deployed according to the manufacturer's recommendations and protocol with slight modification of incubation temperature to ensure optimal GFP folding. Instead of 37°C the

mixture was incubated at 32°C for 3 h. Afterwards, GFP fluorescence was recorded on microtiter plates using a Fluoroskan Ascent Microplate Fluorometer (excitation at 485 nm, emission at 538 nm; ThermoScientific). The mean fluorescence of negative controls was subtracted from the means of tested and control samples and percentages from control were calculated. A minimum of three experiments were performed, and statistical difference was calculated using Microsoft Excel *t*-test.

DNA binding

DNA melting temperature studies. CT-DNA (Sigma Aldrich, France) was dissolved and dialyzed overnight in water prior to use. Tested compounds were dissolved in DMSO (10 mM stock solutions), aliquoted and stored at -20°C to then be temporarily diluted at $10 \mu\text{M}$ in 1 ml of BPE buffer (6 mM Na_2HPO_4 , 2 mM NaH_2PO_4 , 1 mM EDTA, pH 7.1) and incubated (analyzed sample) or not (reference sample) with $20 \mu\text{M}$ of CT-DNA (drug/DNA ratio = 0.5). The absorbance of DNA was measured at 260 nm in quartz cells using an Uvikon 943 spectrophotometer thermostatted with a Neslab RTE111 cryostat every minute over a range of 20 to 100°C with an increment of 1°C per min. The melting temperature (T_m) values were obtained from the midpoint of the hyperchromic transition obtained from first-derivative plots. The variation of melting temperature (ΔT_m) was measured by subtracting the melting temperature measurement of $20 \mu\text{M}$ of CT-DNA incubated alone (control T_m) from that obtained with DNA incubated with increasing concentrations of the various tested compounds ($\Delta T_m \text{ values} = T_{m[\text{Drug+DNA}]} - T_{m[\text{DNA alone}]}$).

UV/visible and circular dichroism (CD) spectrometries

The UV/visible spectra were recorded from 230 nm to 430 nm in a quartz cuvette of 10 mm path length using an Uvikon XL spectrophotometer and referenced against a cuvette containing BPE. Increasing concentrations of CT-DNA (from 10 to $100 \mu\text{M}$ with $10 \mu\text{M}$ steps and then from 100 to $200 \mu\text{M}$ with steps of $20 \mu\text{M}$ of base pairs) were added in both the drug ($20 \mu\text{M}$ in BPE buffer) and the reference (BPE buffer alone) cuvettes and the spectra were recorded stepwise. For CD spectra, CT-DNA ($50 \mu\text{M}$) was incubated with or without (control) a increasing concentrations of the tested drugs (from 1 to $50 \mu\text{M}$) in BPE in a quartz cell of 10 mm path length. The CD spectra were collected from 480 to 230 nm using a J-810 Jasco spectropolarimeter at a controlled temperature of 20°C fixed by a PTC-424S/L peltier type cell changer (Jasco) essentially as described previously.²⁶

Topoisomerase I-mediated DNA relaxation and topoisomerases cleavage assays

Topoisomerase I-mediated DNA relaxation experiments were performed as previously described²⁷ with graded concentrations of the tested compounds incubated with supercoiled pUC19 plasmid prior to the addition of human topoisomerase I (4 units, Topogen, USA) for 45 min at 37°C in relaxation buffer. Addition of SDS (0.25%) and proteinase K ($250 \mu\text{g ml}^{-1}$) for a 30 min incubation at 50°C stopped the reaction. The DNA forms were separated on a 1% agarose gel without ethidium bromide

for 2 h at 120 V in TBE buffer. Gels were stained post-electrophoresis in an ethidium bromide containing-bath, washed and photographed under UV light. Topoisomerase I DNA cleavage assays were performed in the same condition but samples being loaded on a 1% agarose gel containing ethidium bromide. Topoisomerase II DNA cleavage assays were performed as described.¹⁶ Camptothecin (CPT, 20 μM) and etoposide (50 μM) were used as poisons for topoisomerase I and II, respectively.

DNase I footprinting

The 265 bp DNA fragment was obtained from *EcoRI* and *PvuII* double digestion of the pBluscript plasmid (Stratagene, La Jolla, CA) followed by 3'-end labeled at the *EcoRI* site upon incorporation of α -[³²P]-dATP (3000 Ci mmol⁻¹, PerkinElmer, France) by Klenow enzyme for 30 min at 37 °C. After separation on a 6% native polyacrylamide gel, the portion of the gel containing the 265 bp radio-labeled DNA fragment was cut off from the gel, crushed, dialyzed overnight and filtered through a 0.22 μm membrane (Millipore). DNA fragments were finally precipitated from ethanol, dried and dissolved in an appropriate amount of MQ water. DNase I footprinting experiments were performed essentially as previously described.²⁷ The 265 bp radio-labeled DNA fragment was incubated with increasing concentrations of the tested compounds (15 min at 37 °C) prior to mild digestion for 4 min with DNase I (0.002 unit per ml) in reaction buffer (20 mM NaCl, 2 mM MgCl₂, 2 mM MnCl₂, pH 7.3). The reaction was stopped by freeze-drying, lyophilisation and subsequent dissolution in 4 μl of denaturing loading buffer (80% formamide solution containing tracking dyes). The DNA samples were then heated at 90 °C for 4 min, chilled on ice for another 4 min and separated on denaturing 8% polyacrylamide gels containing 8 M urea for 90 min at 65 W in TBE buffer (89 mM Tris base, 89 mM boric acid, 2.5 mM Na₂EDTA, pH 8.3). After migration, gels were soaked in 10% acetic acid, transferred to Whatman 3 MM paper and dried under vacuum at 80 °C to be exposed on a storage screen, and the results were collected using a Molecular Dynamics STORM 860. Each base was localized from comparison with the bands from dimethyl-sulfate (DMS) and piperidine treatment revealing purines with a preference for guanines (strong cut) over adenines (weaker cuts) and is referred to on gels as G+a-track.

Acknowledgements

We greatly appreciate the financial support of the Croatian Ministry of Science Education and Sports (Projects 125-0982464-1356, 098-0982464-2514) and the bilateral Hubert Curien partnership between Croatian and French institutions (Cogito program) as the Egide Project no. 24765PH. We are thankful to Dr Igor Weber for help with confocal microscopy experiments. M. H. David-Cordonnier is grateful to the Ligue Nationale Contre le Cancer (Comité du Pas-de-Calais, Septentrion), the Association Laurette Fugain and the Association pour la Recherche sur le Cancer for grants; the Institut pour la Recherche sur le Cancer de Lille (IRCL), the CHRU de Lille and the Région Nord/Pas-de-Calais for a PhD fellowship to Raja

Nhili and the IRCL for technical expertise (Sabine Depauw) and post-doctoral fellowship (Raja Nhili).

References

- 1 S. Demirayak, U. Abu Mohsen and A. Cagri Karaburun, *Eur. J. Med. Chem.*, 2002, **37**, 255–260.
- 2 M. Hranjec, M. Kralj, I. Piantanida, M. Sedić, L. Šuman, K. Pavelić and G. Karminski-Zamola, *J. Med. Chem.*, 2007, **50**, 5696–5711.
- 3 Y. Bansal and O. Silakari, *Bioorg. Med. Chem.*, 2012, **20**, 6208–6236.
- 4 L. W. Deady, T. Rodemann, G. J. Finlay, B. C. Baguley and W. A. Denny, *Anti-Cancer Drug Des.*, 2000, **15**, 339–346.
- 5 M. Demeunynck, C. Bailly and W. D. Wilson, in *D.N.A. and R.N.A. Binders*, Wiley-VCH, Weinheim, 2002.
- 6 W. D. Wilson, B. Nguyen, F. A. Tanious, A. Mathis, J. E. Hall, C. E. Stephens and D. W. Boykin, *Curr. Med. Chem.: Anti-Cancer Agents*, 2005, **5**, 389–408.
- 7 R. B. Silverman, *The Organic Chemistry of Drug Design and Drug Action*, Elsevier Academic Press, 2nd edn, 2004.
- 8 R. Martínez and L. Chacón-García, *Curr. Med. Chem.*, 2005, **12**, 127–151.
- 9 P. Vivas-Mejía, J. L. Rodríguez-Cabán, M. Díaz-Velázquez, M. G. Hernández-Pérez, O. Cox and F. A. Gonzalez, *Mol. Cell. Biochem.*, 1997, **177**, 69–77.
- 10 C. Bailly, *Curr. Med. Chem.*, 2000, **7**, 39–58.
- 11 M. F. Brana, M. Cacho, A. Gradillas, B. de Pascual-Teresa and A. Ramos, *Curr. Pharm. Des.*, 2001, **7**, 1745–1780.
- 12 K. Hirano, Y. Oderaotoshi, S. Minataka and M. Komatsu, *Chem. Lett.*, 2001, 1262–1263.
- 13 V. B. Kovalska, D. V. Kryvorotenko, A. O. Balanda, M. Y. Losytsky, V. P. Tokar and S. M. Yarmoluk, *Dyes Pigm.*, 2005, **67**, 47–54.
- 14 N. Perin, M. Hranjec, G. Pavlović and G. Karminski-Zamola, *Dyes Pigm.*, 2011, **91**, 79–88.
- 15 M. Hranjec, I. Piantanida, M. Kralj, L. Šuman, K. Pavelić and G. Karminski-Zamola, *J. Med. Chem.*, 2008, **51**, 4899–4910.
- 16 (a) M. Hranjec, G. Pavlović, M. Marjanović, M. Kralj and G. Karminski-Zamola, *Eur. J. Med. Chem.*, 2010, **45**, 2405–2417; (b) N. Perin, L. Uzelac, I. Piantanida, G. Karminski-Zamola, M. Kralj and M. Hranjec, *Bioorg. Med. Chem.*, 2011, **19**, 6329–6339.
- 17 M. F. Braña, J. M. Castellano, G. Keilhauer, A. Machuca, Y. Martin, C. Redondo, E. Schlick and N. Walker, *Anti-Cancer Drug Des.*, 1994, **9**, 527–538.
- 18 D. Gunther and R. Erckel, DE 2640 549 A1.
- 19 A. Masta, P. J. Gray and D. R. Phillips, *Nucleic Acids Res.*, 1995, **23**, 3508–3515.
- 20 Q. Zhou, Y. Qu, J. B. Mangrum and X. Wang, *Chem. Res. Toxicol.*, 2011, **24**, 402–411.
- 21 R. P. Hertzberg, M. J. Caranfa and S. M. Hecht, *Biochemistry*, 1989, **28**, 4629–4638.
- 22 K. A. Heminger, S. D. Hartson, J. Rogers and R. L. Matts, *Arch. Biochem. Biophys.*, 1997, **344**, 200–207.
- 23 R. L. Momparler, M. Karon, S. E. Siegel and F. Avila, *Cancer Res.*, 1976, **36**, 2891–2895.

- 24 P. Peixoto, C. Bailly and M. H. David-Cordonnier, *Methods Mol. Biol.*, 2010, **613**, 235–256.
- 25 A. Lansiaux, L. Dassonneville, M. Facompré, A. Kumar, C. E. Stephens, M. Bajic, F. Tanious, W. D. Wilson, D. W. Boykin and C. Bailly, *J. Med. Chem.*, 2002, **45**, 1994–2002.
- 26 T. Lemster, U. Pindur, S. Depauw, G. Lenglet, C. Dassi and M. H. David-Cordonnier, *Eur. J. Med. Chem.*, 2009, **44**, 3235–3252.
- 27 P. Peixoto, Y. Liu, S. Depauw, M. P. Hildebrand, D. W. Boykin, C. Bailly, W. D. Wilson and M. H. David-Cordonnier, *Nucleic Acids Res.*, 2008, **36**, 3341–3353.